Journal of Catalysis **211,** 540–547 (2002)
doi:10.1006/jcat.2002.3777

Influence of Steam Activation on Pore Structure and Acidity of Zeolite Beta: An Al *K* Edge XANES Study of Aluminum Coordination

J. A. van Bokhoven,*[,1,2] D. C. Koningsberger,* P. Kunkeler,† and H. van Bekkum†

*Debye Institute, Department of Inorganic Chemistry and Catalysis, Utrecht University, Sorbonnelaan 16, 3508 TB Utrecht, The Netherlands; and †Department of Organic Chemistry and Catalysis, Delft University of Technology, Julianalaan 136, 2628 BL Delft, The Netherlands

Received June 13, 2002; revised July 29, 2002; accepted July 31, 2002

The effect of steam activation on the aluminum coordination in zeolite NH_4-beta was investigated by means of quantitative analysis of Al *K* edge XANES spectra. Framework tetrahedral aluminum is converted to octahedral aluminum after calcination and steaming, a process that, at the same time, removes NH_3 and brings about Lewis acidity. After mild activation, this octahedral aluminum can revert to the tetrahedral state by NH_3 treatment while preserving long-range ordering. This implies that structural changes are fully reversible. Intense steaming causes irreversible changes in the structure of the zeolite: some of the tetrahedrally coordinated aluminum is distorted and octahedrally coordinated aluminum is present in the zeolite. NH_3 treatment of intensely steamed zeolite beta results in the reversal of all octahedrally coordinated aluminum to the tetrahedrally coordinated structure, while medium range ordering around some of the tetrahedral aluminum is lost. N_2 physisorption experiments indicate that intense steaming creates clefts or mesopores in the zeolite crystallites, resulting in a decrease in the length of the diffusion pathways of the reactants. This explains, at least in part, the enhanced activity of zeolite beta in the Lewis acid (Al-)catalyzed Meerwein–Ponndorf–Verley (MPV) reaction after intense steaming.

Key Words: **zeolite beta; Al *K* edge XAFS; aluminum coordination; zeolite activation; pore structure.**

INTRODUCTION

Zeolites find wide application as catalysts and catalyst supports. Today, zeolites are increasingly used in fine-chemical applications. Zeolite beta is a typical example of a zeolite with high activity in liquid-phase fine-chemical reactions. The framework aluminum in zeolites is tetrahedrally coordinated. However, based on ^{27}Al NMR, it has been proposed that, after activation, octahedrally coordinated aluminum, which is linked to the framework, is formed (1–5). This was first observed for zeolite beta, but similar behavior has been reported for ZSM-5 (6) and Y zeolite (7). Based upon ^{27}Al MAS NMR, this octahedral aluminum reverted to tetrahedral coordination after ammonia treatment at 100°C (1) or after ion exchange (8). It has been proposed for zeolite beta that framework aluminum can be octahedrally coordinated, depending on the ligands that are coordinated to the aluminum. Hence, framework aluminum may then function as a Lewis acid center (9).

A quantitative ^{27}Al multiple quantum MAS NMR study on zeolite beta, treated at different temperatures and steam content, showed the quantitative reversal of framework aluminum to octahedral coordination (10). The high resolution of the NMR data in that study enabled a distinction to be made between different crystallographic T sites in the zeolite, which behaved differently with respect to reversal to octahedral coordination. Moreover, it was shown that the removal of aluminum from the framework was correlated with the formation of octahedral framework aluminum.

A recent study suggests that the flexibility of the framework of zeolite beta is responsible for the *para*-selective nitration of toluene (11). An octahedrally coordinated aluminum attached to the framework was proposed to be in an intermediate state during this *regio*-selective reaction. More evidence for Lewis activity of the framework of zeolite beta was provided by temperature-programmed ammonia desorption (TPAD). These experiments suggest the presence of Lewis acid sites, which are associated with framework-related octahedral aluminum (12).

Many catalytic reactions benefit from the activation of the zeolite. These activation procedures generally consist of dealumination of the zeolite, either by steaming and/or by leaching with an acid or base. To elucidate the effect of steam activation, in-depth knowledge of the structure of the zeolites as a function of the steam treatment is required.

In a previous paper, the activity for the Meerwein–Ponndorf–Verley (MPV) selective conversion of 4-*tert*-butylcyclohexanone to *cis*-4-*tert*-butylcyclohexanol (9) was related to the aluminum coordination in zeolite beta. It was shown by ^{27}Al MAS NMR that activation of the zeolite at 450°C leads to the appearance of octahedrally coordinated

[1] Current address: Laboratory for Technical Chemistry, ETH Hönggerberg, CH-8093 Zurich, Switzerland.

[2] To whom correspondence should be addressed. E-mail: j.a.vanbokhoven@tech.chem.ethz.ch.

0021-9517/02 $35.00

aluminum (accompanied by the creation of Lewis acidity), but only to low activity for the MPV reaction. Upon steaming at 550°C, the reaction rate was increased dramatically. ^{27}Al MAS NMR revealed the presence of octahedrally coordinated aluminum. It was also shown that water is crucial for the creation of Lewis acidity. The following points, however, remained unanswered. (i) What is the influence of steam treatment on Lewis acidity? (ii) Is the Lewis acid site framework or nonframework aluminum? (iii) Why does the activity increase after steaming at 550°C?

Al XANES spectra enables quantitative determination of the coordination of aluminum (13); the different aluminum coordinations can be distinguished by their specific lineshapes. None of the aluminum escapes detection by XANES. This is a generally occurring phenomenon in ^{27}Al MAS NMR, which depends on the correct choice of magnetic field strength, the spinning speed, and the pulse program to minimize the chance of aluminum escaping detection (14–16). Moreover, Al XANES is sensitive to structural ordering up to 15 Å around the absorber aluminum atom (17). Recent instrumental developments (18, 19) have made *in situ* characterization (i.e., at elevated temperature and pressure) at the Al *K* edge possible.

This paper presents an Al *K* edge XANES study on zeolite beta and a nitrogen physisorption analysis. Framework tetrahedral aluminum can be converted to octahedral aluminum on steaming. Intense steaming irreversibly changes the structure of the zeolite: Medium-range ordering around part of the tetrahedral aluminum is lost. Nitrogen physisorption (*t*-plot) analysis reveals that severe steaming creates clefts or mesopores in the crystallites, thereby decreasing the length of the diffusion pathways of the reactants.

EXPERIMENTAL

Zeolite Synthesis

Macrocrystalline zeolite beta (1–2 μm) was prepared according to Kunkeler *et al.* (20). The as-synthesized beta was carefully washed with water until pH 7. Debris, possibly formed during the cooling of the synthesis mixture, was removed by washing with a 0.025 M Na_2H_2EDTA solution at room temperature. The macrocrystalline beta was contaminated by a small amount of mordenite (less than 1%) (20).

Calcination and Activation

The calcination was performed in a horizontal glass tube using 10 g zeolite. First, the obtained beta was calcined in an atmosphere of pure ammonia from ambient temperature to 400°C (1°C/min, 6 h, 400°C). The resulting white material was sodium exchanged overnight using a 1 M NaCl solution (100 ml/g zeolite) under reflux. The thus-obtained zeolite was calcined at 120°C in oxygen containing approximately 1% ozone, followed by a calcination step at 400°C (1°C/min, 6 h, 400°C) in oxygen. Threefold ion exchange with a 0.1 M NH_4NO_3 solution at room temperature finally gave the parent sample (NH_4)beta1 (9).

Activation of small amounts of (NH_4)beta1 (100–200 mg) was conducted in a small glass tube mounted horizontally in a tubular oven. To obtain a shallow calcination bed, the samples were well distributed. Activation of all the samples was performed at 1°C/min.

The parent sample (NH_4)beta1 was heat treated for 1 h at 450°C in a stream of dry nitrogen. The resulting sample is referred to as (H)beta1 450(1 h)d. (H)beta1 550(3d)w30 formed after 3 days of steam treatment of (NH_4)beta1 at 550°C. Low water pressure was maintained at 4.2 kPa in a saturator operating at 30°C. (H)beta1 450(1 h)–NH_3 and (H)beta1 550(3d)w30–NH_3 were formed by separate treatments of (H)beta1 450(1 h)d and (H)beta1 550(3d)w30, with NH_3 at 100°C for 24 h.

All the samples were checked by XRD, ^{27}Al MAS NMR, and N_2 physisorption and were found to be "pure" zeolite beta. N_2 physisorption was measured using a Micromeritics ASAP 2400 instrument, and the samples were outgassed in vacuum at 250°C for 24 h before measurement.

XAFS Experiments

XAFS measurements were performed at the Al *K* edge (1560 eV) at station 3.4 at the SRS in Daresbury (UK). The *in situ*, low-energy XAFS cell, ILEXAFS, was used (18, 19). This ILEXAFS setup consists of a small stainless-steel chamber placed inside a large vacuum vessel. The atmosphere inside the small chamber can be controlled by varying the pressure, temperature, and gas flow. Detection was carried out using fluorescence (with a gas proportional counter) and electron yield (measuring drain current) simultaneously. Only the fluorescence data are presented here, because the electron yield data give identical results. Samples were pressed into wafers. The I_0 signal was measured by the drain current flowing from a Cu mesh. Data treatment, like normalization, was performed according to standard procedures (21). Different aluminum coordinations can be deduced from the X-ray absorption near edge (XANES) by identification of characteristic features in the spectra (13, and references therein).

RESULTS

N_2 Physisorption Isotherms

Table 1 lists the samples and the micropore volumes obtained from the N_2 physisorption experiments. Figure 1 shows the N_2 physisorption isotherms of (NH_4)beta1 and (H)beta1 550(3d)w30. The high microporosity of both samples and the hysteresis at $P/P_0 = 0.45$ in (H)beta1 550(3d)w30 are clearly visible. The hysteresis of the parent sample (NH_4)beta1 is not visible and is only very small

TABLE 1

Results of N_2 Physisorption of the Zeolite Beta Samples

Sample	Micropore vol. (cm^3/g)	Hysteresis
(NH_4)beta1	0.25	No
(H)beta1 450(1 h)d	0.25	Very small
(H)beta1 450(1 h)d–NH_3	n.d.	n.d.
(H)beta1 550(3d)w30	0.24	Yes
(H)beta1 550(3d)w30–NH_3	0.23	Yes

for the activated sample (H)beta1 450(1 h) (not shown). Apparently, significant mesopore formation occurred only in (H)beta1 550(3d)w30. The creation of mesopores in the steamed zeolite was accompanied by an increase of ~1 to 3 m^2/g in external surface, as obtained from *t*-plot analysis.

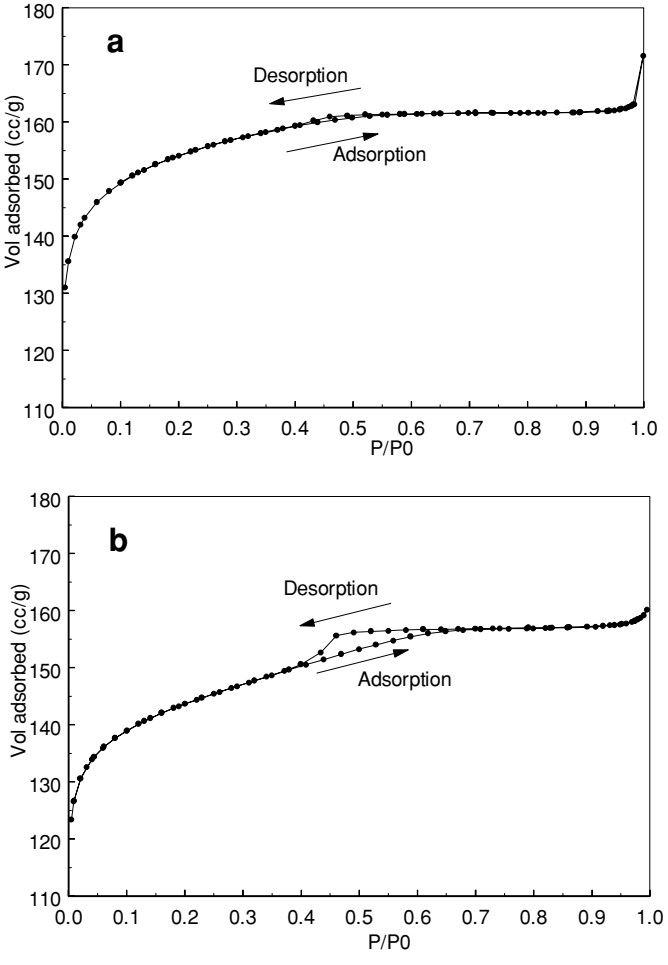

FIG. 1. N_2 adsorption and desorption isotherms on (a) (NH_4)beta1 and (b) (H)beta1 550(3d)w30 showing hysteresis of the intensely steamed zeolite beta.

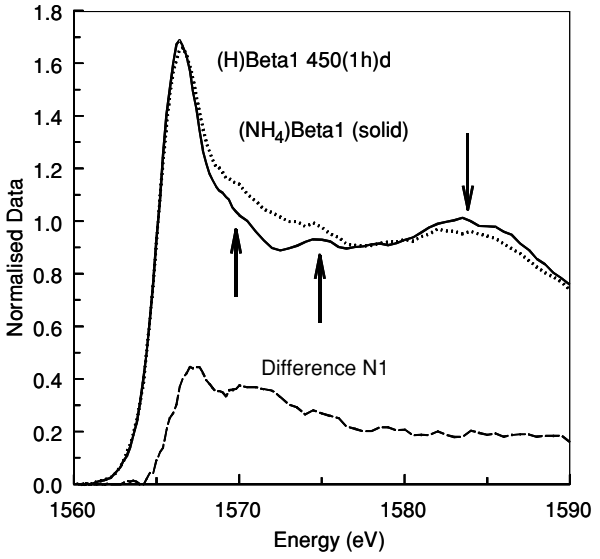

FIG. 2. Al *K* edge fluorescence data of (NH_4)beta1 (solid line) and (H)beta1 450(1 h)d (dotted line). The difference (N1) between the two spectra is also shown (dashed line; see text for details). The arrows indicate characteristic features of spectra of tetrahedrally coordinated aluminum.

According to the IUPAC classification (22–24), the mesopores in the steamed sample (H)beta1 550(3d)w30 are slit shaped. The micropore volumes of all the samples are comparable (Table 1). Activation and steaming causes a small decrease in BET-micropore surface area and micropore volume. Although *t*-plot analysis of microporous zeolite structures does not yield absolute values, the observed relative numbers are assumed to be reliable.

XANES of Al K Edge

The fluorescence data of the Al *K* edge of (NH_4)beta1 are represented by a solid line in Fig. 2. The spectrum of (NH_4)beta1 shows the characteristic lineshape of tetrahedrally coordinated aluminum (13). A sharp white line is visible at 1566 eV. Arrows indicate characteristic features at 5 and 10 eV above the absorption edge, which has energy E_0 and is defined as the inflection point in the edge. For the tetrahedral coordination, the energy of the absorption edge is about $E_0 = 1565$ eV. The shape of these peaks as well as the shape and intensity of the white line are determined by ordering up to 15 Å around the absorber atom (17, 25). A loss of ordering would be evident from the loss of these two features. The broad peak at $E_0 = +19$ eV (see arrow in Fig. 2) is indicative of tetrahedral aluminum. This peak is determined mainly by the structure of the first (tetrahedral) coordination sphere around the absorber atom and its energy is related to the Al–O bond length (25).

The short-activated sample (H)beta1 450(1 h)d (Fig. 2, dotted line) shows differences in the range of 0 to 25 eV above the absorption edge. A higher intensity is seen at up to about $E_0 = +14$ eV. The maximum intensity of the edge

is shifted to higher energy compared to that of (NH_4)beta1. The broad component at $E_0 = +19$ eV indicates that most of the aluminum in the sample did not change and is still tetrahedrally coordinated, although its intensity is clearly diminished. The difference between (H)beta1 450(1 h)d and the parent sample can be isolated from the spectrum:

$$\text{Difference (N1)} = \text{(H)beta1 450(1 h)d} - \text{N1} \times (NH_4)\text{beta1}. \quad [1]$$

The normalization factor N1 is a measure of the amount of tetrahedral aluminum in (H)beta1 450(1 h)d and was progressively increased, starting at $N = 0$, until none of the characteristic features for tetrahedral aluminium was visible in the difference spectrum. The intensity at 1566 eV is regarded as an indicator of the presence of tetrahedral aluminum. (Spectra of octahedral aluminum are not very intense at this energy.) The resulting difference (N1) spectrum is indicated by a dashed line in Fig. 2 and was obtained at a value of N1 = 0.75. Note the difference in the peak position of the difference (N1) spectrum (1568 eV) and the spectrum of the (NH_4)beta1 sample. Figure 3 presents a comparison of the difference (N1) spectrum (solid line) on an absolute scale with the spectrum of corundum (dotted line), a reference compound for (distorted) octahedral aluminum. In general, Al *K* edge XANES spectra of

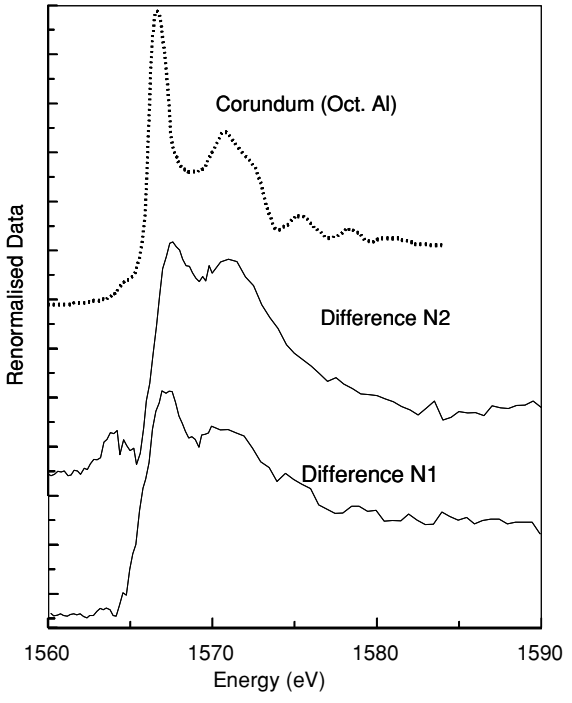

FIG. 3. The difference (N1) spectrum (solid line) of (NH_4)beta1 and (H)beta1 450(1 h)d compared to corundum as a reference material, with octahedrally coordinated aluminum (dotted line), showing the same characteristic features. The difference (N2) spectrum of (H)beta1 550(3d)w30 and (H)beta1 550(3d)w30–NH_3 is added (see text for details).

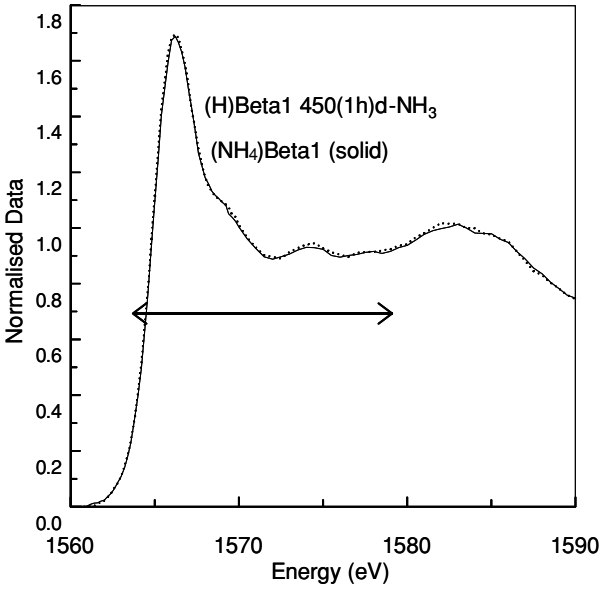

FIG. 4. Al *K* edge fluorescence data of (H)beta1 450(1 h)d–NH_3 (solid line) and (NH_4)beta1 (dotted line). The arrow indicates the energy range of the spectrum that is determined by ordering up to 15 Å around the aluminum.

samples with an octahedral aluminum coordination display very characteristic features (13). The increased symmetry in octahedral compared to tetrahedral aluminum results in higher intensity at the edge region of the octahedral aluminum spectra. Similarities between the two spectra are evident (Fig. 3): A split absorption edge (with peaks at about 1568 and 1572 eV, respectively), characteristic of octahedrally coordinated aluminum, is visible in both spectra. The edge of an octahedrally coordinated aluminum shifts by ~2 eV to higher energy compared to that of tetrahedral aluminum, as is visible in the difference (N1) spectrum in Fig. 2. It can, therefore, be concluded that the difference (N1) spectrum is indicative of octahedrally coordinated aluminum. Al XANES enables also the quantitative determination of different coordination types, assuming identical absorption coefficients for the different coordinations (26). By comparing the relative surface areas under the spectra, defined by N1, the amount of octahedrally coordinated aluminum in (H)beta1 450(1 h)d is calculated to be ~25%. No indication for other coordinations is found.

The Al *K* edge XANES spectrum of (H)beta1 450(1 h)d–NH_3 (dotted line), the beta that was activated for 1 h at 450°C and treated with ammonia at 100°C for 24 h, was compared to the spectrum of the parent material, (NH_4)beta1 (Fig. 4, solid line). The two spectra are identical within the limits of accuracy, and hence, the coordination of aluminum in both samples is the same. From this it follows that in the ammonia-treated sample, the octahedral aluminum reverted quantitatively to the original tetrahedrally coordinated aluminum. Moreover, the arrow in Fig. 4 represents the energy range of the spectrum that is sensitive to

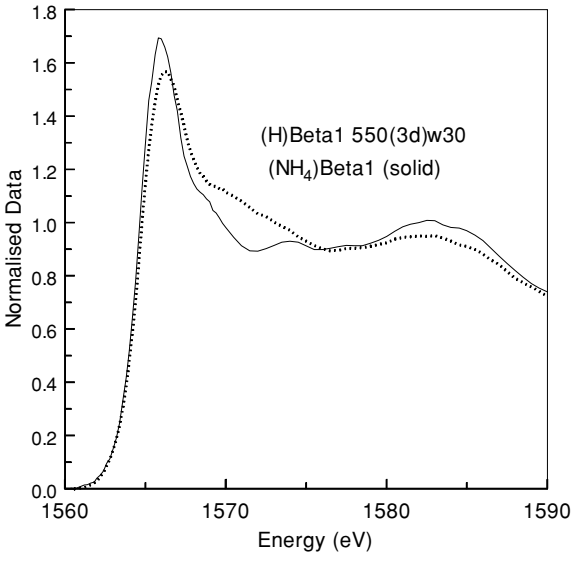

FIG. 5. Al *K* edge fluorescence data of (NH_4)beta1 (solid line) and the intensely steamed (H)beta1 550(3d)w30 (dotted line).

ordering up to 15 Å around the aluminum atom (17, 25). This region did not change in relation to the parent sample, indicating that in both samples the aluminum has an identical geometrical environment up to 15 Å.

Figure 5 shows the effect of intense steaming on the zeolite beta and a comparison of the Al *K* edge spectra of the parent (NH_4)beta1 sample (solid line) and the intensely steamed (H)beta1 550(3d)w30 sample (dotted line). The spectrum of (H)beta1 550(3d)w30 resembles the spectrum of (H)beta 450(1 h)d (Fig. 2); however, the fine structure at $E_0 = +5$ and $E_0 = +10$ eV is lost. The diminished intensity of the white line as well as the broad component at $E_0 = +19$ eV points to the disappearance of some tetrahedrally coordinated aluminum. In comparing Figs. 2 and 5, it is concluded that intensely steamed beta also contains octahedrally coordinated aluminum as well as tetrahedral aluminum.

Figure 6 shows the spectra of the parent sample (NH_4)beta1 (solid line) and the ammonia-treated (H)beta1 550(3d)w30–NH_3 sample (dotted line). It is evident that in this case, too, the octahedrally coordinated aluminum reverted to tetrahedrally coordinated aluminum, as is mainly indicated by the decrease in intensity in the range 1568 to 1575 eV compared with the spectrum of (H)beta1 550(3d)w30 (Fig. 5). Moreover, the region $E_0 = +0$ to +15 eV above the edge, which is determined by ordering up to 15 Å (indicated by the arrow in Fig. 6), is less well structured compared with the parent material. This indicates a loss of ordering around part of the tetrahedrally coordinated aluminum.

To obtain an impression of the amount of octahedral aluminum in the intensely steamed sample, the tetrahedral aluminum contribution to the spectrum is subtracted from the spectrum of the steamed sample (Fig. 5, dotted line), using the ammonia-treated steamed beta as a tetrahedral reference:

$$\text{Difference (N2)} = \text{(H)beta1 550(3d)w30} - \text{N2} \times \text{(H)beta1 550(3d)w30–NH}_3. \quad [2]$$

It is assumed that the tetrahedral coordinations are approximately the same in both samples. However, the ammonia-treated sample contains some tetrahedral aluminum, which resulted from the reversal of octahedral aluminum back to tetrahedral, as is also deduced from ^{27}Al (MQ) MAS NMR. This reversed tetrahedral aluminum is not present in the steamed sample. However, the quantity of the octahedral part in the spectrum can be estimated. Figure 3 shows the difference (N2) spectrum (solid), obtained at N2 = 0.78, with regard to the spectrum of corundum (dotted) and difference (N1). In this case too, the difference spectrum is typical of an octahedral coordination. However, by comparing the difference (N1) and the difference (N2) spectra it is clear that the relative intensity of the two dominating peaks in the spectra is different. This suggests a different (average) octahedral coordination in the intensely steamed zeolite beta.

The percentage of octahedral aluminum in (H)beta1 550(3d)w30 is estimated to be ~22%, based on the intensities below the spectra.

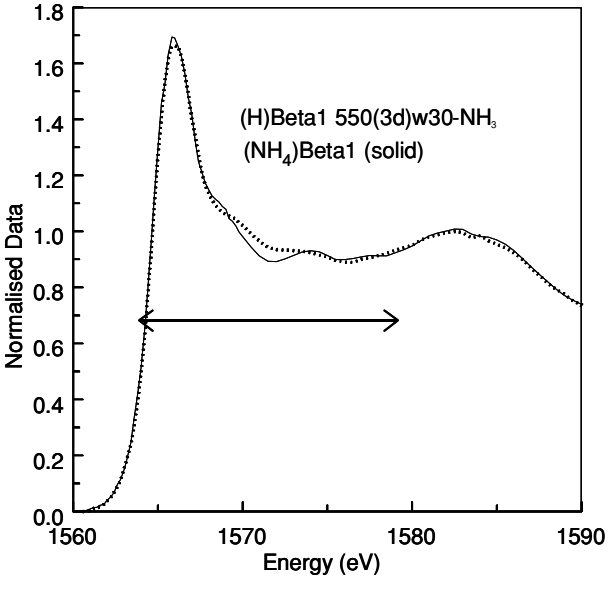

FIG. 6. Al *K* edge fluorescence data of (H)beta1 550(3d)w30–NH_3 (solid line) and (NH_4)beta1 (dotted line). The arrow indicates the energy range of the spectrum that is determined by long-range ordering around the aluminum.

DISCUSSION

Al Coordination as a Function of the Activation Treatments

According to Al *K* edge XANES no aluminum escapes detection. Simulations estimate that because of the high quality of the data, the presence of about 5% distorted tetrahedral aluminum can be distinguished from nondistorted tetrahedral aluminum. Al *K* edge XANES does not indicate any three-coordinated aluminum. Three-coordinated aluminum is expected to be visible at a lower edge position in the Al *K* edge XANES spectra than is tetrahedrally coordinated aluminum (13), showing that Al XANES is even more sensitive (only a few percent would be detected) to the presence of this coordination.

The quantitative analysis shows that tetrahedrally coordinated aluminum in (H)beta1 450(1 h)d–NH_3 cannot be distinguished from the tetrahedral aluminum in the parent sample, (NH_4)beta1. The overlapping Al *K* edge spectra demonstrate that the long-range order (<15 Å around the absorber) is indistinguishable in both samples (Fig. 4). This clearly indicates that there is an identical coordination within a 15-Å radius of the aluminum atoms in both samples, showing a complete reversal of coordination after ammonia treatment. This confirms the presence of octahedrally coordinated aluminum attached to the framework (1–6, 10), which can revert completely to tetrahedrally coordinated framework aluminum. In our previous ^{27}Al MQ MAS NMR study (10), we showed that the reversed aluminum has an isotropic chemical shift identical to that of the parent material; this was interpreted as complete restoration of aluminum to identical framework positions.

Steaming at 550°C clearly reveals the appearance of different types of aluminum species, both tetrahedral and octahedral. Hydrolysis of framework aluminum most likely occurred, a process that is associated with a loss of framework aluminum. A treatment with NH_3 causes all the octahedral aluminum to revert to the tetrahedral coordination. However, as indicated by the arrow in Fig. 6, part of the fine structure has been lost. This unambiguously indicates a loss of ordering around some of the aluminum atoms and indicates the presence of an amorphous phase, probably silica–alumina.

Table 2 presents the coordinations of aluminum as determined from the Al *K* edge XANES spectra. It is indicated as to whether or not these species are likely to be framework species.

Pore Structure after Activation

N_2 physisorption experiments show a very similar micropore volume for the parent and (steam) activated zeolite beta (Table 1), indicating that the micropore structure is largely unchanged after steaming. However, the sample steamed at 550°C, (H)beta1 550(3d)w30, shows a hysteresis, which is characteristic of slit-shaped pores (type B), according to the IUPAC classification (22). It is proposed that small mesopores or clefts are created in the crystallites of the zeolite beta, keeping the micropore structure largely intact. The large crystallites of (NH_4)beta1 are cleaved into smaller clusters of crystallites.

TABLE 2

Al Coordinations from Al *K* Edge XANES

Sample	Tetrahedral Al	Octahedral Al
(NH_4)beta1	Framework	None
(H)beta1 450(1 h)d	Framework	Framework
(H)beta1 450(1 h)d–NH_3	Framework	None
(H)beta1 550(3d)w30	Framework and nonframework	Framework and nonframework?
(H)beta1 550(3d)w30–NH_3	Framework and nonframework	None

The formation of mesopores and the increase in the external surface area suggest partial destruction of the crystallites. The loss of ordering around part of the aluminum, as shown by the Al *K* edge XANES data of the intensely steamed beta (Figs. 5 and 6), may well have originated from the aluminum located in or near the clefts.

Consequences for Lewis Acidic Activity

Activation of zeolites may influence their activity. As shown by the Meerwein–Ponndorf–Verley (MPV) reaction, the activated (NH_4)beta1 showed Lewis acid activity after calcination at 450°C (9). This activity increased significantly after steaming at 550°C. Longer steaming at 550°C increased the activity, reaching a plateau of maximal activity after about 2 days of steaming (9). As previously indicated, it was reported that the framework octahedral aluminum is associated with Lewis acidity for ZSM-5 (6) and zeolite beta (12). Partial hydrolysis of the Al–O–Si bonds was proposed, which was reversed after exchange with NH_4^+ or treatment with gaseous NH_3. Moreover, the flexibility of the framework aluminum was suggested to play a role in the *para*-selective nitration of toluene over zeolite beta (11). The reaction products formed a framework-connected octahedral aluminum species, as shown by ^{27}Al MAS NMR. This species was proposed to be responsible for the *regio*-selectivity of this reaction over zeolite beta.

Analogously, we propose that the Lewis acid activity for the MPV reaction in zeolite beta is associated with the ability of the framework to create octahedral aluminum. It has been shown that the MPV reaction occurs inside the pores of the zeolite (27). The limited size of the zeolitic pores forces the *cis*-isomer to be the dominant

product (in all cases >94%). This selectivity is generated by the limited size of the pores and/or the curvature of the pores.

The framework octahedral site is created by the formation of tetrahedral aluminum in H-beta through removal of NH_3 and subsequent addition of water to create octahedral aluminum in the framework of zeolite beta (7, 19). Likewise, a catalytic cycle can be initiated by adding a ketone and the H-donor 2-propanol in the MPV reaction to the tetrahedral aluminum (9). Al *K* edge XANES did not reveal any evidence of the presence of any other coordination except for framework tetrahedral and octahedral aluminum after activation at 450°C. No three-coordinated aluminum, which could function as a Lewis acid site, was detected under the measurement conditions.

Steaming at 550°C leads to a large increase in activity (9) as well as to a loss of local ordering around aluminium atoms, as shown by the Al *K* edge XANES spectra. From N_2 physisorption experiments it is concluded that the micropore structure remains intact. Small clefts or mesopores are also created in the crystallites of the zeolite beta. These cracks shorten the diffusion pathways to the framework active sites of the framework. Crystallites of different sizes showed different activity in the MPV reaction, indicating a diffusion-limited reaction (9). Cleaving the crystallites will lead to a significant increase in site availability. It is, therefore, concluded that after steaming, alleviation of diffusion limitations, at least partly, explains the observed enhanced activity.

In summary, activation of zeolite (NH_4-) beta at 450°C creates Lewis activity, which is associated with the ability of framework tetrahedral aluminum to form octahedral aluminum in the zeolite framework. A large increase in activity is found after steaming at 550°C for a longer period. The active sites show an enhanced participation, because of better access through the creation of mesopores or clefts in the crystallites of the zeolite beta.

CONCLUSIONS

The coordination of aluminum species in zeolite beta can be followed quantitatively as a function of activation using Al *K* edge XAFS. At 450 and 550°C, (steam) activation creates Lewis acid sites associated with the framework. These Lewis active centers are proposed to be associated with framework aluminum, as shown by the *regio*-selective activity in the Lewis-catalyzed Meerwein–Ponndorf–Verley (MPV) reaction for zeolite beta activated at 450°C. The active site is created upon thermal activation of (NH_4)-beta, thus removing NH_3. Addition of water gives the octahedral aluminum site. This octahedral aluminum reverts to tetrahedral framework aluminum after an ammonia treatment at 100°C, restoring the local structure around the aluminum within a radius of 15 Å.

An intensive steam treatment causes irreversible changes in the structure of the zeolite, in addition to creating framework octahedral aluminum. Such severe conditions probably cause some of the aluminum to be extracted from the framework and to leave its original framework position; hence, reinsertion into the framework is not possible. A loss of medium-range ordering around some of the tetrahedral aluminum was found, probably due to aluminum in amorphous silica–alumina. Moreover, N_2 physisorption experiments show that the crystallites contain mesopores that are interpreted as clefts in the crystallites. These mesopores increase the external surface of the crystallites and make the created internal Lewis acid sites more accessible to the reactants in the MPV reaction.

ACKNOWLEDGMENTS

Dr. Andy Smith is thanked for his help during the measurements on beamline 3.4 of the SRS Daresbury. Measurements took place within the scope of Contract 37410. We thank the SRS for providing this beam time.

REFERENCES

1. Bourgeat-Lami, E., Massiani, P., Di Renzo, F., Espiau, P., Fajula, F., and Des Courières, T., *Appl. Catal.* **72**, 139 (1991).
2. Jia, C., Massiani, P., and Barthomeuf, D., *J. Chem. Soc. Faraday Trans.* **89**, 3659 (1993).
3. Beck, L., and Haw, J. F., *J. Phys. Chem.* **99**, 1075 (1995).
4. de Ménorval, L. C., Buckermann, W., Figueras, F., and Fajula, F., *J. Phys. Chem.* **100**, 465 (1996).
5. Kirisci, I., Flego, C., Pazzuconi, G., Parker, W. O., Jr., Millini, R., Perego, C., and Bellussi, G., *J. Phys. Chem.* **98**, 4627 (1994).
6. Woolery, G. L., Huehl, G. H., Timken, H. C., Chester, A. W., and Vartuli, J. C., *Zeolites* **19**, 288 (1997).
7. Wouters, B. H., Chen, T.-H., and Grobet, P. J., *J. Am. Chem. Soc.* **120**, 11419 (1998).
8. Yang, C., and Qinhua, X., *Zeolites* **19**, 404 (1997).
9. Kunkeler, P. J., Zuurdeeg, B. J., van der Waal, J. C., van Bekkum, H., van Bokhoven, J. A., and Koningsberger, D. C., *J. Catal.* **180**, 234 (1998).
10. van Bokhoven, J. A., Koningsberger, D. C., Kunkeler, P., van Bekkum, P., and Kentgens, A. P. M., *J. Am. Chem. Soc.* **122**, 12842 (2000).
11. Haouas, M., Bernasconi, S., Kogelbauer, A., and Prins, R., *Phys. Chem. Chem. Phys.* **3**, 5067 (2001).
12. Kuehl, G. K., Kyung, H., and Timpken, C., *Microporous Mesoporous Mater.* **35–36**, 521 (2000).
13. van Bokhoven, J. A., Sambe, H., Ramaker, D. E., and Koningsberger, D. C., *J. Phys. Chem. B* **103**, 7557 (1999).
14. Kraus, H., Prins, R., and Kentgens, A. P. M., *J. Phys. Chem.* **100**, 16336 (1996).
15. Fyfe, C. A., Bretherton, J. L., and Lam, L. Y., *Chem. Commun.* **17**, 1575 (2000).
16. Van Bokhoven, J. A., Roest, A. L., Nachtegaal, G. H., Kentgens, A. P. M., and Koningsberger, D. C., *J. Phys. Chem. B* **104**, 6743 (2000).
17. Cabaret, D., Sainctavit, P., Ildefonse, Ph., and Flank, A.-M., *J. Phys. Condens. Matter* **8**, 3691 (1996).
18. Van Bokhoven, J. A., van der Eerden, A. M. J., Smith, A. D., and Koningsberger, D. C., *J. Synchrotron Rad.* **6**, 201 (1999).
19. van der Eerden, A. M. J., van Bokhoven, J. A., Smith, A., and Koningsberger, D. C., *Rev. Sci. Instrum.* **71**(9), 3260 (2000).

20. Kunkeler, P. J., Moeskops, D., and van Bekkum, H., *Microporous Mater.* **11**, 313 (1997).
21. Sayers, D. E., and Bunker, B. A., *in* "X-Ray Absorption: Principles, Applications, Techniques of EXAFS, SEXAFS and XANES" (D. C. Koningsberger and R. Prins, Eds.), p. 211. Wiley, New York, 1987.
22. Sing, K. S. W., *Pure Appl. Chem.* **54**, 2201 (1982).
23. De Boer, J. H., *in* "The Dynamical Character of Adsorption," p. 155. Clarendon, Oxford, 1953.
24. Broekhoff, J. C. P., and De Boer, J. H., *in* "Proceedings of the International Symposium on Surface Area Determination" (D. H. Everett and R. H. Ottewill, Eds.), p. 97. Buttersworth, London, 1969.
25. van Bokhoven, J. A., Sambe, H., Ramaker, D. E., and Koningsberger, D. C., *J. Phys. Condens Matter* **13**, 10247 (2001).
26. Shimizu, K., Kato, Y., Yoshida, T., Yoshida, H., Satsuma, A., and Hattori, A., *Chem. Commun.* 1681 (1999).
27. Creyghton, E. J., Ganeshie, S. D., Downing, R. S., and van Bekkum, H., *J. Mol. Catal. A* **115**, 457 (1997).